

# Multipole order and global/site symmetry in the hidden order phase of URu<sub>2</sub>Si<sub>2</sub>

Michi-To Suzuki<sup>1,2</sup> and Hiroaki Ikeda<sup>3</sup>

<sup>1</sup>RIKEN Center for Emergent Matter Science (CEMS), Wako, Saitama 351-0198, Japan

<sup>2</sup>CCSE, Japan Atomic Energy Agency, 5-1-5 Kashiwanoha, Kashiwa, Chiba 277-8587, Japan

<sup>3</sup>Department of Physics, Ritsumeikan University, Kusatsu 525-8577, Japan

(Dated: October 22, 2014)

On the basis of group theory and the first-principles calculations, we investigate high-rank multipole orderings in URu<sub>2</sub>Si<sub>2</sub>, which have been proposed as a genuine primary order parameter in the hidden order phase below 17.5K. We apply Shubnikov group theory to the multipole ordered states characterized by the wave vector  $\mathbf{Q}_0 = (0, 0, 1)$  and specify the global/site symmetry and the secondary order parameters, such as induced dipole moments and change in charge distribution. We find that such antiferroic *magnetic* multipole orderings have particularly advantageous to conceal the primary order parameter due to preserving high symmetry in charge distribution. Experimental observations of the induced low-rank multipoles, which are explicitly classified in this paper, will be key pieces to understand the puzzling hidden order phase.

PACS numbers: 71.20.Gj, 71.27.+a, 75.30.-m, 75.50.Ee

## I. INTRODUCTION

Recently,  $f$  electron compounds have drawn considerable interest, stimulated by observations of exotic ordered ground states forming at low temperatures. The richness of  $f$  electron physics can be attributed to their multiple degrees of freedom in the presence of strong spin-orbit interaction as well as strong electron-electron Coulomb interactions. A striking example is formation of multipole order (MPO), in which spin-orbital space of  $f$  electrons has main role to establish the physical states with strongly correlated electrons. While recent findings of MPO in the  $f$ -electron compounds promise to exotic materials with unprecedented functions, the complex constitution of the microscopic quantum states makes it difficult to identify the ordered states experimentally. A well known example of the MPO formation is the ground state of NpO<sub>2</sub>. While the order parameter had been enigma for fifty years,<sup>1,2</sup> it has been recently clarified that the ordering is characterized by the  $3\mathbf{q}$  antiferroic (AF) structure of T<sub>2</sub> multipoles,<sup>3-5</sup> which is a high-rank multipole without dipolar magnetic moment. Another example is the formation of the hidden order (HO) phase in URu<sub>2</sub>Si<sub>2</sub>, where various type of the high-rank multipoles have been suggested as promising primary order parameters by theoretical studies.<sup>6-17</sup>

The HO state accompanied by the second order phase transition at  $T_{\text{HO}}=17.5\text{K}$  in URu<sub>2</sub>Si<sub>2</sub> has been an object of study over 30 years since its discovery.<sup>18-20</sup> The phase transition is associated with abrupt change in the bulk properties at  $T_{\text{HO}}$  and is accompanied by large reduction of the carrier number.<sup>21,22</sup> The tiny magnetic moments experimentally observed in the HO phase are currently considered to be an extrinsic effect from inhomogeneity of the crystal,<sup>23-29</sup> and there is little consensus about the order parameter which characterizes the HO phase.<sup>30</sup> The conventional AF magnetic phase appear accompanied by the first order phase transition at  $P_c \sim 1.5\text{GPa}$ .<sup>27,31,32</sup> Inelastic neutron experiments have reported that the both

ordered phases are associated with the identical wave vectors  $\mathbf{Q}_0=(0,0,1)$ .<sup>33</sup> First-principles calculations also predict the  $\mathbf{Q}_0$  as the ordering vector from the calculations of  $\mathbf{Q}$  dependent multipole susceptibility.<sup>16</sup> Interestingly, the de Haas-van Alphen (dHvA) measurements under pressure observe very little change in the frequencies from the HO phase to the ordinary AF magnetic phase, which indicate that the both phases have the very similar Fermi surfaces.<sup>34-36</sup> Fermi surfaces calculated with the local spin density approximation (LSDA) for the AF magnetic dipolar states well explain the dHvA frequencies,<sup>37-39</sup> and the energy bands are shown to be qualitatively unchanged for the difference of the local multipoles, including the magnetic dipoles.<sup>16</sup> In this regard, electronic structure analysis also support the  $\mathbf{Q}_0$  as the characteristic wave vector of the HO phase. Meanwhile, the  $\mathbf{Q}$  vector characterizing HO phase transition is still open question,<sup>40-43</sup> and a direct experimental probe of the characteristic  $\mathbf{Q}$  vector, for instance, by detecting the correspondent electronic/magnetic diffraction pattern is still important to clarify the HO state.

Possible signatures from the HO state have been reported in some experimental studies. The Ru-NQR and Si-NMR experiments have reported a broadening of the spectrum below the transition temperature,<sup>44,45</sup> which indicates the presence of the internal fields induced with the HO. The elastic anomalies observed at  $T_{\text{HO}}$  can be related to the induced quadrupole moments accompanied by the phase transition.<sup>46,47</sup> These experimental observations, however, are considered to be secondary effects parasitic on the genuine order parameter of the HO state. Due to the extremely subtle changes, it is always difficult to conclude whether the secondary effects are intrinsic or extrinsic. Recent magnetic torque measurement reports broken in-plane 4-fold symmetry below  $T_0$ , suggesting the HO state has, so called, a nematic property of the electronic state.<sup>48</sup> This observation strongly confines symmetries in the HO phase, and therefore can be crucial clue to identify the genuine order parameter in the

HO phase. Some recent experiments may have also been providing useful clues to confine possible symmetries of the HO states.<sup>49,50</sup>

In order to understand these experimental observations, it is very useful to clarify the global/site symmetry and the corresponding secondary order parameters in high-rank MPO states. Also, such classification would further stimulate experimental studies. In this paper, we investigate the symmetry related properties of the AF-MPO states of URu<sub>2</sub>Si<sub>2</sub> by applying Shubnikov group theory, which indicates full symmetry information concerning the electric/magnetic degrees of freedom in the ordered states. Classification of the AF-MPO states provides common ground for discussion of the hidden order in URu<sub>2</sub>Si<sub>2</sub>. For instance, we obtain knowledge regarding secondary order parameters allowed to appear at each atomic site in several AF-MPO states, which is crucial to experimentally identify the HO state.

As discussed later, the charge distribution of AF-magnetic MPO states in URu<sub>2</sub>Si<sub>2</sub> are clearly distinguished from the magnetic distribution in terms of symmetry, and the magnetic AF- $\Gamma^-$  MPO states always preserve the symmetry of the charge distribution higher than that of the corresponding electric AF- $\Gamma^+$  MPO states. On this point, occurrence of the AF-magnetic MPO states works better for concealing the ordered states by preserving the charge symmetries higher than ones of the electric MPO state.

In Sec. II symmetry of the MPO states in URu<sub>2</sub>Si<sub>2</sub> are discussed based on Shubnikov group theory. After providing some definition regarding local multipoles defined on U atoms in Sec. II A, we discuss the global symmetry of the MPO states in Sec. II B. Features of secondary order parameters, of which the definition through this paper would be provided, in the AF-MPO states is discussed in Sec. II C. In Sec. II D the local site symmetries of Ru and Si sites are investigated to provide crucial information for indirect observation of the MPO states such as NQR/NMR experiment. In Sec. III we provide the computational analysis of  $A_2^-$  and  $E^-$  MPO states, in which the magnetic moments can be contained in terms of the symmetry, based on the first-principles approach to estimate amount of the secondary order parameters in these MPO states. It would be shown that the magnetic moments in the HO state are extremely small even if the symmetry allows the presence.

## II. SYMMETRIC PROPERTIES OF AF-MPO STATES IN URu<sub>2</sub>Si<sub>2</sub>

### A. Multipole theories of URu<sub>2</sub>Si<sub>2</sub>

The multipole moments of URu<sub>2</sub>Si<sub>2</sub> are classified according to IREP of the  $D_{4h}$  point group to which the U sites belong, i.e.  $\Gamma=A_{1g}, A_{2g}, B_{1g}, B_{2g}$ , or  $E_g$ , assuming the presence of the space inversion symmetry in the HO phase. We would omit the index  $g$  hereafter. The

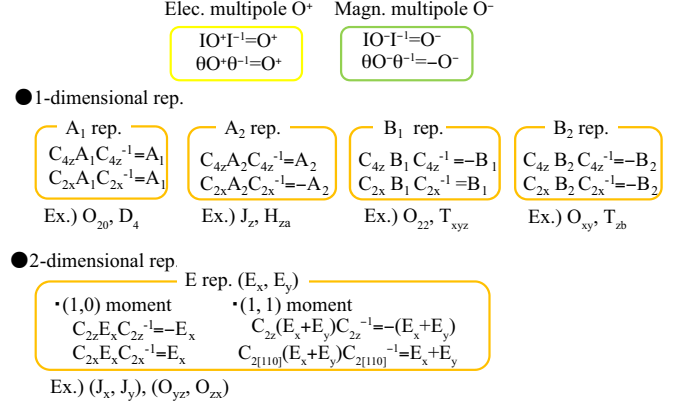


FIG. 1: Local transformation property of multipoles in a  $D_4$  point symmetry site. The multipole operators are represented as the symbol of each irreducible representation, whose examples are shown below each box. The symbols of multipole operators are defined following TABLE S1 in the supplementary information of Ref. 16.

multipole moments are further divided by parity for the time reversal operation, and the multipole which have the even/odd parity for the time reversal symmetry would be indicated by the index  $+/-$ , such as  $\Gamma^+$  or  $\Gamma^-$ . For instance, the magnetic dipole  $J_z$  belongs to  $A_2^-$  multipole. Note that the multipole with E-IREP, proposed as primary order parameter in our previous study,<sup>16</sup> has two-dimensional IREP, and the symmetry depends on the linear combination of  $(E_x, E_y)$ , see Fig. 1. We take, through this paper, the two dimensional components  $(E_x, E_y)=(1,1)$ , which is consistent with the nematic properties observed experimentally.<sup>48,51,52</sup>

We focus on, through this paper, the MPOs which are characterized by the commensurate wave vector  $\mathbf{Q}=\mathbf{Q}_0=(0,0,1)$ , which is considered to be a plausible possibility from the previous experimental and theoretical works.<sup>16,33</sup> As a matter of fact, the rotation symmetries which distinguish the type of multipoles as in Fig. 1 can be present only with the translation symmetries preserved in the order characterized by, except  $\mathbf{Q}=\mathbf{0}$ , the minimal commensurate wave vector, and one of the main arguments in this paper, suggesting the high symmetry of the AF-MPO states, is therefore not held with other finite  $\mathbf{Q}$ . The fact that the HO phase is characterized by the wave vector  $\mathbf{Q}_0=(0,0,1)$  leads to a simple consequence that the local order parameters aligned on U sites with simple type-I AF structure, in which the multipole moments on the body-center uranium sites are *opposite* from ones on the other uranium sites, in the HO phase. Here, *opposite* multipole moment is defined as the multipole moment of which the expectation value has opposite sign. The second order phase transition at  $T_{HO}$  restrict the symmetry of the HO phase to a subgroup of the paramagnetic space group above  $T_{HO}$ . The

Landau phenomenological analysis further indicates that the bi-critical point of the paramagnetic, the HO, and the AF magnetic (AFM) phases on the P-T phase diagram<sup>32,53–56</sup> is explained from the fact that the symmetry of the HO phase is different from that of the ordinary AFM phase.<sup>9,40</sup> These facts are consistent that the HO state is characterized by type-I AF structure of a multipole moment with symmetry *different* from that of the ordinary AFM state, and we hereafter consider symmetry in type-I AF MPO states in URu<sub>2</sub>Si<sub>2</sub>.

### B. Shubnikov space groups of AF-MPO states in URu<sub>2</sub>Si<sub>2</sub>

Shubnikov group theory can provide common ground for characterizing the electric/magnetic symmetries in the paramagnetic, the AFM, and the HO phases of URu<sub>2</sub>Si<sub>2</sub> in a unified manner. In general, the Shubnikov space group (SSG)  $\mathcal{M}$  are classified in relation to the ordinary space group (OSG)  $\mathcal{G}$  into two broad categories depending on the presence or absence of anti-unitary part as follows:

$$\mathcal{M} = \mathcal{G}, \quad (1)$$

$$\mathcal{M} = \mathcal{G} + \theta\{R | \tau\}\mathcal{G}, \quad (2)$$

where  $\theta$  is time reversal operator and  $\{R | \tau\}$  is a space group element with the rotation operator  $R$  accompanied by the extra translation  $\tau$ . Note that the  $\{R | \tau\}$  is not necessary to be an element of the unitary group  $\mathcal{G}$  in eq. (2). For instance, the symmetry of paramagnetic phase is characterized by a paramagnetic space group  $\mathcal{G}_{\text{PM}} \otimes T$ ,<sup>57</sup> where the  $\mathcal{G}_{\text{PM}}$  is the OSG of the crystal structure, which is  $I4/mmm$  (No. 139) in case of URu<sub>2</sub>Si<sub>2</sub>, and  $T = \{E, \theta\}$ . The paramagnetic space group corresponds to the SSG of eq. (2) with  $\{R | \tau\} = \{E | \mathbf{0}\}$ . As we will see in the case of the AF-MPO states of URu<sub>2</sub>Si<sub>2</sub>, the global symmetry of MPO state is determined by the local transformation property of the order parameter for the rotation operators of space group (See Fig. 1).

The SSG of Eq. (1), which is characterized by absence of the anti-unitary part, is called Fedrov group.<sup>57</sup> For instance, the  $3\mathbf{q}$  type magnetic multipolar state of NpO<sub>2</sub> belongs to Fedrov group of eq. (1) since any anti-unitary operations do not preserve the non-collinear alignment of the magnetic multipoles. The SSG of HO phase in URu<sub>2</sub>Si<sub>2</sub> belongs to a subgroup of the paramagnetic space group from the discussion of Sec. II A, and the possible AF-MPO states of URu<sub>2</sub>Si<sub>2</sub> belong to the SSG of eq. (2). This is because the time reversal operation, which keeps electric multipoles and flips magnetic multipoles, preserve the global symmetry in case of electric MPO and with an extra translation to the body center sites,  $\tau_{\text{AF}}$ , in magnetic MPO.

As discussed in sec. II C, the different categories of the SSG for the AF-MPO states in NpO<sub>2</sub> and in URu<sub>2</sub>Si<sub>2</sub> clearly distinguish the property of secondary order parameters allowed in these ordered states.

The electric and magnetic MPO states in URu<sub>2</sub>Si<sub>2</sub> are thus clearly distinguished through the anti-unitary part of SSG as following:

$$\mathcal{M}_{\Gamma\pm} = \mathcal{G}_{\Gamma} + \theta\{E | \tau^{\pm}\}\mathcal{G}_{\Gamma}, \quad (3)$$

where  $\tau^{+} = \mathbf{0}$  for electric MPO and  $\tau^{-} = \tau_{\text{AF}}$  for magnetic MPO, respectively. The space group  $\mathcal{G}_{\Gamma}$  corresponds to  $P4/mmm$  (No.123),  $P4/mnc$  (No.128),  $P4_2/mmc$  (No.131),  $P4_2/mnm$  (No.136), and  $Cmce$  (No.64) for  $\Gamma = A_1, A_2, B_1, B_2$ , and  $E$  multipolar states, respectively. Note that the space groups  $\mathcal{G}_{\Gamma}$  except the  $\mathcal{G}_{A_1}$  belong to nonsymmorphic space groups with extra translation  $\tau_{\text{AF}}$ . Since the electric MPOs do not break magnetic symmetry, the full symmetry can be described by the OSG  $\mathcal{G}_{\Gamma}$  within electric degrees of freedom, and the electric symmetries have been investigated in earlier work.<sup>13</sup> The magnetic symmetries correspond to the MPO states of magnetic multipoles which belong to one-dimensional IREPs are also explored in the magnetic neutron study.<sup>58</sup> Our present work has developed the symmetry analysis so as to describe possible electric/magnetic multipolar states in the same framework, clarifying the structure of global symmetries of the electric and magnetic MPO states.

### C. Secondary order parameters in magnetic MPO states

Order parameters characterize symmetry breaking from a paramagnetic state to ordered states. In the ordered states, there often appear additional changes induced by the presence of the primary order parameters, such as structural distortion in magnetic orderings. Such secondarily induced quantities are compatible with symmetry in the ordered states. Considering the global/site symmetry in the ordered states, we can classify the presence of the induced secondary order parameters. Knowledge of such secondary order parameters is crucially important in high-rank MPO states, since it is very difficult to detect high-rank multipole moments experimentally. The SSG classification of the MPO states is available for identification of all of the secondary order parameters in the MPO states.

Electric multipole moments induced as the secondary order parameters often provides crucial information to identify the magnetic MPO, since the reduced charge symmetry can be detected through change in the electronic diffraction pattern. Furthermore, detection of electric quadrupole moments are generally easier than detection of the higher rank magnetic multipoles by the experiment such as resonant X-ray or ultrasonic sound wave. The symmetry of the electric component in magnetic MPO is, in general, derived from the SSG. In case of the magnetic ordered states which belongs to Fedrov group, the OSG of charge distribution is indicated by  $\mathcal{G}$ , and the symmetry belongs to the same one with the magnetic distribution as seen in Eq. (1). For instance,

Paramagnetic phase									
$\mathcal{M}$					$\mathcal{G}_C$				
$I4/mmm1'$					$I4/mmm$				
AF-Electric MPO phase									
IREP	$\mathcal{M}$	$\mathcal{G}_C$	Time reversal	4-fold rotation	IREP	$\mathcal{M}$	$\mathcal{G}_C$	Time reversal	4-fold rotation
$A_1^+$	$P4/mmm1'$	$P4/mmm$	Preserved	Preserved	$A_1^-$	$P14/mmm$	$I4/mmm$	Broken	Preserved
$A_2^+$	$P4/mnc1'$	$P4/mnc$	Preserved	Preserved	$A_2^-$	$P14/mnc$	$I4/mmm$	Broken	Preserved
$B_1^+$	$P4_2/mmc1'$	$P4_2/mmc$	Preserved	Preserved	$B_1^-$	$P14_2/mmc$	$I4/mmm$	Broken	Preserved
$B_2^+$	$P4_2/mnm1'$	$P4_2/mnm$	Preserved	Preserved	$B_2^-$	$P14_2/mnm$	$I4/mmm$	Broken	Preserved
$E^+$	$Cmce1'$	$Cmce$	Preserved	Broken	$E^-$	$C_{Amce}$	$Fmmm$	Broken	Broken

TABLE I: SSG of the magnetic symmetries,  $\mathcal{M}$ , in the AF-MPO states of  $\text{URu}_2\text{Si}_2$  and the CSG for the charge distribution,  $\mathcal{G}_C$ . The notation of SSG follows Ref. 57. The presence of time reversal and four fold rotational symmetries are also indicated.

because the  $3\mathbf{q}$  AF magnetic structure in  $\text{NpO}_2$  belongs to Fedrov group, the OSG of the MPO ground states<sup>59</sup> already provides full symmetry of the magnetic MPO states of  $\text{NpO}_2$  from eq. (1). In this case, the electric multipoles which belong to the same symmetry with the primary magnetic multipole is induced as the secondary

order parameter. Actually, resonant X-ray and NMR experiments concluded the magnetic multipolar state of  $\text{NpO}_2$  by detecting the *electric* quadrupole order induced with the primary higher-rank magnetic MPO,<sup>3-5</sup> considering the experimental observations of the breaking of time reversal symmetry.<sup>60,61</sup>

In case of the magnetic states which belong to Eq. (2), the symmetry of the charge distribution is indicated by the OSG  $\mathcal{G} + \{R | \tau\}\mathcal{G}$  where the symbols are already defined in Eq. (2), since the time reversal operation does not affect to the charge component. We will refer to the OSG of charge distribution as charge space group (CSG)  $\mathcal{G}_C$  hereafter. From above discussion, the symmetry of charge distribution in each AF-MPO state of  $\text{URu}_2\text{Si}_2$  is identified. The SSG of the magnetic symmetry in the AF-MPO states and the corresponding CSG are listed in Table I. It is found from the table that the magnetic MPO characterized by  $A_1^-$ ,  $A_2^-$ ,  $B_1^-$ , and  $B_2^-$ -MPOs, which

belong to one dimensional IREPs, have the same CSG with that of paramagnetic states, i.e.  $\mathcal{G}_C = I4/mmm$ . This fact leads to a conclusion that these AF-MPO states do not induce any charge deformation which break the symmetry of the paramagnetic states. In other words, identification of these MPO states is possible only by detecting the symmetry breaking caused by the magnetic distribution.

The AF  $E^\pm$  multipolar states break the four-fold rotational symmetry as shown in the table I. When the multipole moments are induced with the two dimensional components preserving the symmetry higher, such as  $(E_x, E_y) = (1, 1)$ , the  $E^\pm$  MPO states have orthorhombic conventional cell, yet the primitive unit cell is the same with that of the other multipolar states, see Fig. 2. Operation of two fold rotation along the tetragonal axis,  $C_{2z}$ , transform the E multipoles to the *opposite*, and the unitary operator  $\{C_{2z} | \tau_{AF}\}$  therefore preserve the AF- $E$  MPO states equivalent. Okazaki et al. refer the fourfold symmetry breaking as *electronic nematic*.<sup>48</sup> The AF- $E^-$  MPO state, interestingly, permit an electronic deformation to the ferroic  $B_2^+$  MPO, which contain the *ferroic*  $O_{xy}$  quadrupole order, since the charge distribution in the AF- $E^-$  MPO states belongs to the space group  $Fmmm$  (No. 69). This electronic deformation is symmetrically equivalent to that reported in the iron-based superconductor  $\text{BaFe}_2\text{As}_2$ .<sup>62</sup> The recent highly accurate X-ray diffraction measurement using high-resolution synchrotron X-ray has reported the observation of the reduction of electric symmetry in the HO phase of  $\text{URu}_2\text{Si}_2$ .<sup>63</sup>

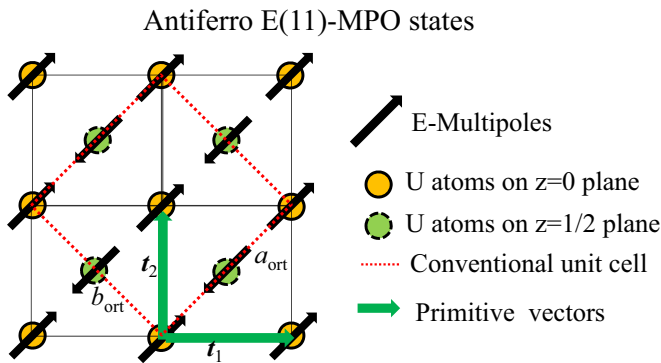


FIG. 2: Schematic picture of the relation between the primitive and the conventional unit cell in AF-E MPO induced with the two dimensional components  $(E_x, E_y) = (1, 1)$ .



### D. Atomic site symmetries in AF-MPO states

The local symmetries of Ru and Si atomic sites in the HO phase are important to identify the ordered states through the observation of the secondarily induced electric/magnetic distribution on the atomic sites.<sup>44,45</sup> The local magnetic/electric symmetry of MPO states are also derived from the SSG in the ordered states.

Table II shows the site symmetries of all atomic sites in each AF-MPO state of URu<sub>2</sub>Si<sub>2</sub>. The ordinary point groups for local charge distribution at each atomic site are also found from this table by omitting 1' and the primes (') from the symbols. Since the multipole moments in URu<sub>2</sub>Si<sub>2</sub> is originated from U-*f* electrons, the local symmetries of U sites are equivalent to that of the multipole moments. The magnetic dipoles along the tetragonal axis can be induced on the U and Si atomic sites in the AF-A<sub>2</sub><sup>-</sup> MPO states, to which the ordinary

AFM states belong, and on the Ru sites in the AF-B<sub>2</sub><sup>-</sup> MPO states. Moreover, *in-plane* magnetic dipole moments are allowed in the all of atomic sites in the AF-E<sup>-</sup> MPO states. In these AF-MPO states, the secondarily induced dipole moments can be detected by experimental observation by NQR/NMR experiments although the induced signals may be extremely small.<sup>52,64</sup>

On the other hand, no magnetic dipole moment is induced at any atomic sites in AF-A<sub>1</sub><sup>-</sup> and AF-B<sub>1</sub><sup>-</sup> MPO states. Since these AF-MPO states neither induce any charge deformations which break the symmetry of paramagnetic states as discussed in Sec. II C and as also found in table I and II, identification of these ordered states requires, for experiments, direct detection of the higher rank magnetic multipoles such as magnetic octupole and magnetic triakontadipole in case of the B<sub>1</sub><sup>-</sup> and A<sub>1</sub><sup>-</sup> MPO, respectively (see, e.g., TABLE I in Ref. 14 or TABLE S1 of supplementary information of Ref. 16).

Paramagnetic phase				
Atom	Atomic sites	Local sym.		
U	1	(2a) $4/mmm1'$		
Ru	1	(4d) $\bar{4}m21'$		
Si	1	(4e) $4mm1'$		

AF-Electric MPO phase					AF-Magnetic MPO phase				
Atom	Atomic sites	Local sym.		Mag. moments	Atom	Atomic sites	Local sym.		Mag. moments
$A_1^+$	U	2	$(1a) 4/mmm1' \oplus (1d) 4/mmm1'$	None	U	1	(2a) $4/mmm$	None	
	Ru	1	(4i) $2mm.1'$	None	$A_1^-$	Ru	1	(4d) $\bar{4}'m2'$	None
	Si	2	$(2g) 4mm1' \oplus (2h) 4mm1'$	None	Si	1	(4e) $4mm$	None	
$A_2^+$	U	1	(2a) $4/m..1'$	None	U	1	(2a) $4/mm'm'm'$	$M_z$	
	Ru	1	(4d) $2.221'$	None	$A_2^-$	Ru	1	(4d) $\bar{4}'m'2$	None
	Si	1	(4e) $4..1'$	None	Si	1	(4e) $4m'm'm'$	$M_z$	
$B_1^+$	U	1	(2c) $mmm.1'$	None	U	1	(2a) $4'/mmm'$	None	
	Ru	2	$(2e) \bar{4}m21' \oplus (2f) \bar{4}m21'$	None	$B_1^-$	Ru	1	(4d) $\bar{4}m2$	None
	Si	1	(4i) $2mm.1'$	None	Si	1	(4e) $4'mm'm'$	None	
$B_2^+$	U	1	(2a) $m.mm1'$	None	U	1	(2a) $4'/mm'm'm$	None	
	Ru	1	(4d) $\bar{4}..1'$	None	$B_2^-$	Ru	1	(4d) $\bar{4}m'2'$	$M_z$
	Si	1	(4e) $2.mm1'$	None	Si	1	(4e) $4'm'm'm$	None	
$E^+$	U	1	(4a) $2/m..1'$	None	U	1	(4a) $mm'm'm'$	$M_{x(Ortho)}$	
	Ru	1	(8e) $.2.1'$	None	$E^-$	Ru	1	(8f) $2'22'$	$M_{y(Ortho)}$
	Si	1	(8f) $m..1'$	None	Si	1	(8i) $mm'2'$	$M_{x(Ortho)}$	

TABLE II: Local symmetries of atomic sites in the AF-MPO states. The third column shows number of the non-equivalent atomic sites. The notation of site symmetry basically follows Ref. 65, adding 1' for the pure time reversal operator or prime (') on the symbols corresponding to operators combined with time reversal. Wyckoff letters for CSG are adapted to specify the atomic positions, see also Table I. The magnetic moments of E<sup>-</sup>-MPO, *M<sub>μ</sub>(Ortho)* (*μ*=x, y), are labeled for the *orthorhombic* axis (see Fig. 2), which have relation such as *M<sub>x</sub>(Ortho)* =  $\frac{1}{\sqrt{2}}(M_x + M_y)$ .

### III. COMPUTATIONAL INVESTIGATION OF SECONDARY ORDER PARAMETERS

Recent magnetic torque measurement and high-resolution synchrotron X-ray diffraction measurement

have reported observation of breaking four-fold rotation symmetry in the HO phase.<sup>48,63</sup> Within the multipole

theory, these observations indicate that the order parameters are E-type multipoles. The rather low charge symmetry of AF-E<sup>+</sup> MPO, which are shown in Table I and II, not only for rotation symmetry but also for translation symmetry is likely to be difficult to conceal the order parameters from experimental observations, but it is still a possible candidate in terms of the breaking four-fold symmetry including the observation of split of a X-ray diffraction spot<sup>63</sup> and, possibly, lack of magnetic moments.

Our previous theoretical works have predicted the magnetic E<sup>-</sup> MPO state in the HO phase.<sup>16</sup> In terms of symmetry, the E<sup>-</sup>-MPO states contain in-plane magnetic moments as the member of multipoles, and *why experiments have not detected the in-plane dipole moments so far* is a big issue to be resolved if the AF-E<sup>-</sup>-MPO is the ordered state in the HO phase. To investigate the problem, we have performed the first-principles electronic structure calculations to quantitatively estimate the magnetic moments which can be present in the AF-MPO states. Since the electric/magnetic degree of freedom to describe the multipole moments are included in the local LDA+*U* potentials, the AF-MPO states can be calculated with the LDA+*U* calculations properly considering the global electric/magnetic symmetries.<sup>66,67</sup> The detailed calculation method for the multipole ordered states based on the LDA+*U* method is described in Ref. 67. We used the exchange-correlation functional of Gunnarsson and Lundqvist for the LDA potential.<sup>68</sup> The double-counting term has been chosen as in the around mean field, leaving out the spin dependency of the Hund's coupling part to adapt it for the nonmagnetic LDA part as in the Ref. 67. Earlier theoretical work has estimated the appropriate range of *U* values of URu<sub>2</sub>Si<sub>2</sub> as less than 1 eV.<sup>11</sup> We therefore performed the calculations by changing the *U* values from 0 to 1.0 eV with the Hund's coupling parameter *J*=0.1 eV. The ordered states are calculated under the restriction of SSG for each AF-MPO state.

The multipole moments can be described through the radial function of the local density matrix, calculated as following

$$\rho_{\gamma\gamma'}^{\tau\ell}(r^\tau) = \frac{1}{N} \sum_{\mathbf{k}b} \langle \tau\ell\gamma | \mathbf{k}b \rangle \langle \mathbf{k}b | \tau\ell\gamma' \rangle (r^\tau), \quad (4)$$

where  $\tau$  and  $\ell$  denote the atoms and angular momenta of the orbitals, respectively.  $\gamma$  ( $\gamma'$ ) is an index related to an orbital  $m$  ( $m'$ ) and a spin  $s$  ( $s'$ ).  $\mathbf{k}$  and  $b$  denote wave vector and band index, respectively.  $N$  is the number of  $\mathbf{k}$  points and  $r^\tau$  the radial component of the position vector  $\mathbf{r}^\tau$  measured from atom  $\tau$ . The local multipole moment  $O^\tau$  on a atom is calculated with the local basis set  $\{|\tau\ell\gamma\rangle\}$  inside the MT sphere, following the expression<sup>67</sup>

$$O^\tau = \sum_{\ell} \sum_{\gamma} \sum_{\gamma_1\gamma_2} \int dr^\tau \{r^\tau\}^2 \rho_{\gamma\gamma_1}^{\tau\ell}(r^\tau) O_{\gamma_1\gamma_2}^{\tau\ell} \rho_{\gamma_2\gamma}^{\tau\ell}(r^\tau), \quad (5)$$

where  $O_{\gamma\gamma'}^{\tau\ell}$  denote the matrix elements of the multipole

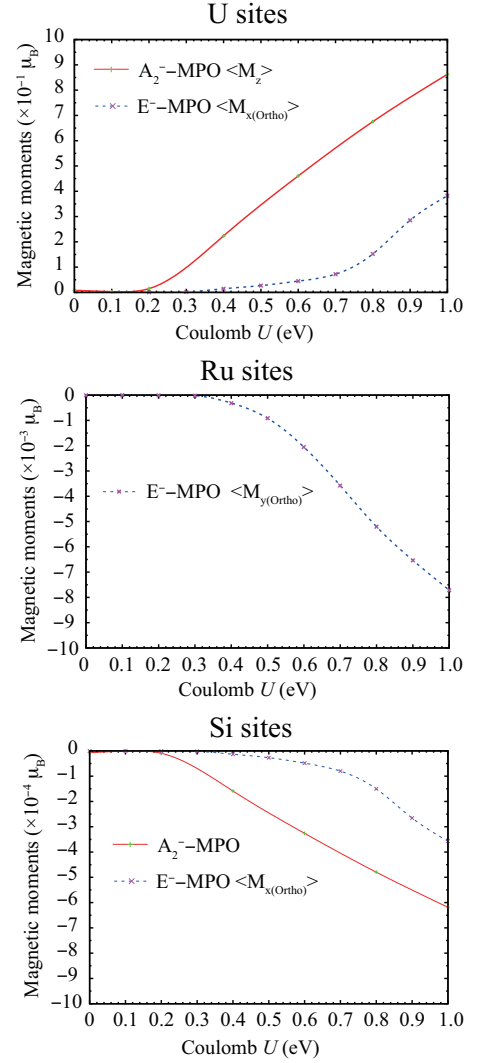


FIG. 3: Calculated magnetic moments symmetrically arrowed to appear on each atomic site in the AF-A<sub>2</sub><sup>-</sup> and the AF-E<sup>-</sup> states. Hund's coupling *J* is chosen as 0.1 eV in the LDA+*U* method.

operator  $\hat{O}^{\tau\ell}$ , whose explicit expressions up to rank-5 are listed in the supplementary information of our previous work.<sup>16</sup> Figure 3 plots magnetic moments on each atomic site in the A<sub>2</sub><sup>-</sup> and E<sup>-</sup> MPO states of URu<sub>2</sub>Si<sub>2</sub> applying the *U* values from 0 to 1 eV. In the symmetry view point, the magnetic moments can be present on U and Si sites in the A<sub>2</sub><sup>-</sup>-MPO, on Ru sites in B<sub>2</sub><sup>-</sup>-MPO, and on all atomic sites in E<sup>-</sup>-MPO states. Meanwhile, our calculations show no finite values for  $\langle M_z \rangle$  moments on Ru atoms in B<sub>2</sub><sup>-</sup>-MPO states for the calculated *U* region. This result shows that the B<sub>2</sub><sup>-</sup> multipoles on U sites, which contain no dipole moment as the constituent, hardly couple with the magnetic dipoles on the Ru sites. In the A<sub>2</sub><sup>-</sup>-MPO states corresponding to AFM phase, the magnetic moments along the tetragonal axis linearly increase with the increased *U* values above

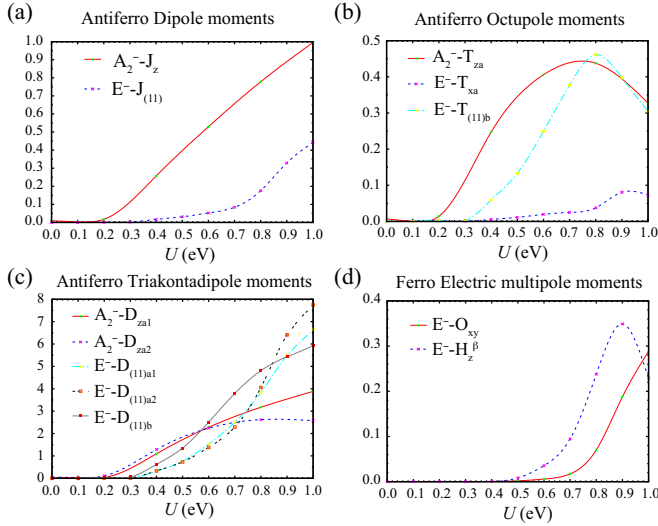


FIG. 4: Absolute values of calculated (a) dipole, (b) octupole, (c) triakontadipole moments induced on uranium sites in the AF- $A_2^-$  and AF- $E^-$  states. The ferroic electric multipolar moments in the  $E^-$  multipolar states are also plotted in (d). The operator expression of multipole moments are defined for the tetragonal axis, and symbols such as  $A_{(11)}$  indicate the multipole moments with the components  $(A_x, A_y)=(1, 1)$  in two dimensional IREP., i.e.  $A_{(11)\alpha} \equiv \frac{1}{\sqrt{2}}(A_{x\alpha} + A_{y\alpha})$ .

0.2eV. Amount of the magnetic moments are  $\sim 10^{-1} \mu_B$ , which is consistent with experimentally observed magnetic moments in the AFM phase under pressure, i.e.  $0.1 \sim 0.4 \mu_B$  for the small range of  $U$  below 0.6eV. On the other hand, the shift of in-plane magnetic moments of  $E^-$ -MPO states is suppressed below 0.7eV and develop linearly above 0.7eV, in which the magnetic moments are at most one order smaller than ones of the  $A_2^-$  states on U atoms. This result shows that the paramagnetic electronic structure around the Fermi level has tiny response for the in-plane magnetic moments, which is consistent with our previous work.<sup>16</sup>

The magnetic moments secondarily induced by the MPO at U sites are also plotted in the Fig. 3. This figure shows that the LDA+ $U$  calculation for the  $E^-$ -MPO states produces the magnetic moments  $\sim 10^{-2} \mu_B$  at U sites,  $\sim 10^{-4} \mu_B$  at Ru sites and  $\sim 10^{-5} \mu_B$  at Si sites for the expected  $U$  values discussed above. There is an obvious trend to leave the induced moments small, as compared with those of AFM states in the appropriate  $U$  range. Although the magnitude of the induced moment on U site may be detectable, it is likely that the effect of electron correlations beyond the Hartree-Fock level in the LDA+ $U$  method makes this value still one-

order smaller, as such effect is important to suppress the in-plane magnetic response in the uniform susceptibility.

Figure 4 shows that, while the development of the in-plane magnetic dipole moments of  $E^-$ -MPO for the  $U$  parameter is considerably smaller than that of  $A_2^-$ -MPO, the higher-rank multipole moments have comparable contribution of octupole moments and larger contribution of triakontadipole moments compared to those of  $A_2^-$ -MPO. We have also confirmed the electric multipolar moments accompanied by the  $E^-$ -MPO is also very little in the AF- $E^-$  MPO states as shown in Fig. 4 (d). Although possible lattice distortions of  $a_{\text{ortho}} \neq b_{\text{ortho}}$ , which is not taken into account in the current results, can slightly enhance the ferroic quadrupole moments, we find the lattice distortion in  $E^-$ -MPO state is extremely small due to the very weak coupling between the quadrupole moments and the lattice system. Nevertheless, the experimental techniques with great sensitivity for the electronic modification such as NQR/NMR<sup>44,45</sup> or ultrasonic sound wave experiments<sup>47,49</sup> may have captured the subtle trace from the reduction of charge symmetry. These results indicate that the magnetic  $E^-$ -MPO states obtain the energy gain not from the dipole moment but from the higher-rank magnetic multipole moments in the small range of  $U$ .

#### IV. SUMMARY

We have investigated the character of the full symmetry in the AF-MPO states as promising candidates of the hidden-order state in  $\text{URu}_2\text{Si}_2$ . On the basis of Shubnikov group theory, the electric/magnetic symmetry in the AF-MPO states has been explicitly identified, and the global and atomic local symmetry have been classified. The AF-MPO states which belong to one dimensional IREPs induce no electric charge deformation, and  $A_1^-$  and  $B_1^-$  MPO states do not allow any induced dipole moments at atomic sites. Although AF- $E^-$  MPO states can induce in-plane AF dipole and ferroic  $B_2^+$  multipoles as the secondary order parameter, our LDA+ $U$  calculations revealed that the magnitude of the secondary order parameters is extremely small in the appropriate interaction parameter range. Further experimental trials to detect possible traces from HO states are strongly encouraged to identify the order parameters.

#### Acknowledgments

We thank S. Kambe, Y. Tokunaga, and T. Takimoto for valuable discussions. This work has been supported by JSPS KAKENHI Grant Number 24540369.

<sup>1</sup> P. Santini, S. Carretta, G. Amoretti, R. Caciuffo, N. Magnani, and G. H. Lander, Rev. Mod. Phys. **81**, 807 (2009).

<sup>2</sup> Y. Kuramoto, H. Kusunose, and A. Kiss, J. Phys. Soc. Jpn. **78**, 072001 (2009).

- <sup>3</sup> J. A. Paixão, C. Detlefs, M. J. Longfield, R. Caciuffo, P. Santini, N. Bernhoeft, J. Rebizant, and G. H. Lander, *Phys. Rev. Lett.* **89**, 187202 (2002).
- <sup>4</sup> Y. Tokunaga, Y. Homma, S. Kambe, D. Aoki, H. Sakai, E. Yamamoto, A. Nakamura, Y. Shiokawa, R. E. Walstedt, and H. Yasuoka, *Phys. Rev. Lett.* **94**, 137209 (2005).
- <sup>5</sup> Y. Tokunaga, D. Aoki, and et al., *Phys. Rev. Lett.* **97**, 257601 (2006).
- <sup>6</sup> P. Santini and G. Amoretti, *Phys. Rev. Lett.* **73**, 1027 (1994).
- <sup>7</sup> F. J. Ohkawa and H. Shimizu, *J. Phys.: Condens. Matter* **11**, L519 (1999).
- <sup>8</sup> P. Fazekas, A. Kiss, and K. Radnóczy, *Prog. Theor. Phys. Suppl.* **160**, 114 (2005).
- <sup>9</sup> A. Kiss and P. Fazekas, *Phys. Rev. B* **71**, 054415 (2005).
- <sup>10</sup> K. Hanzawa and N. Watanabe, *J. Phys.: Condens. Matter* **17**, L419 (2005).
- <sup>11</sup> F. Cricchio, F. Bultmark, O. Grånäs, and L. Nordström, *Phys. Rev. Lett.* **103**, 107202 (2009).
- <sup>12</sup> K. Haule and G. Kotliar, *Nat. Phys.* **5**, 796 (2009).
- <sup>13</sup> H. Harima, K. Miyake, and J. Flouquet, *J. Phys. Soc. Jpn.* **79**, 033705 (2010).
- <sup>14</sup> P. Thalmeier and T. Takimoto, *Phys. Rev. B* **83**, 165110 (2011).
- <sup>15</sup> H. Kusunose and H. Harima, *J. Phys. Soc. Jpn.* **80**, 084702 (2011).
- <sup>16</sup> H. Ikeda, M.-T. Suzuki, R. Arita, T. Takimoto, T. Shibauchi, and Y. Matsuda, *Nat. Phys.* **8**, 528 (2012).
- <sup>17</sup> J. G. Rau and H.-Y. Kee, *Phys. Rev. B* **85**, 245112 (2012).
- <sup>18</sup> T. T. M. Palstra, A. A. Menovsky, J. van den Berg, A. J. Dirkmaat, P. H. Kes, G. J. Nieuwenhuys, and J. A. Mydosh, *Phys. Rev. Lett.* **55**, 2727 (1985).
- <sup>19</sup> M. B. Maple, J. W. Chen, Y. Dalichaouch, T. Kohara, C. Rossel, M. S. Torikachvili, M. W. McElfresh, and J. D. Thompson, *Phys. Rev. Lett.* **56**, 185 (1986).
- <sup>20</sup> W. Schlitz, J. Baumann, B. Pollit, U. Rauchschwalbe, H. Mayer, U. Ahlheim, and C. Bredl, *Z. Phys. B Condens. Matter* **62**, 171 (1986).
- <sup>21</sup> K. Behnia, R. Bel, and et al., *Phys. Rev. Lett.* **94**, 156405 (2005).
- <sup>22</sup> Y. Kasahara, T. Iwasawa, H. Shishido, T. Shibauchi, K. Behnia, Y. Haga, T. D. Matsuda, Y. Onuki, M. Sigrist, and Y. Matsuda, *Phys. Rev. Lett.* **99**, 116402 (2007).
- <sup>23</sup> C. Broholm, J. K. Kjems, W. J. L. Buyers, P. Matthews, T. T. M. Palstra, A. A. Menovsky, and J. A. Mydosh, *Phys. Rev. Lett.* **58**, 1467 (1987).
- <sup>24</sup> T. E. Mason, B. D. Gaulin, J. D. Garrett, Z. Tun, W. J. L. Buyers, and E. D. Isaacs, *Phys. Rev. Lett.* **65**, 3189 (1990).
- <sup>25</sup> E. D. Isaacs, D. B. McWhan, R. N. Kleiman, D. J. Bishop, G. E. Ice, P. Zschack, B. D. Gaulin, T. E. Mason, J. D. Garrett, and W. J. L. Buyers, *Phys. Rev. Lett.* **65**, 3185 (1990).
- <sup>26</sup> M. B. Walker, W. J. L. Buyers, Z. Tun, W. Que, A. A. Menovsky, and J. D. Garrett, *Phys. Rev. Lett.* **71**, 2630 (1993).
- <sup>27</sup> H. Amitsuka, M. Sato, N. Metoki, M. Yokoyama, K. Kuwahara, T. Sakakibara, H. Morimoto, S. Kawarazaki, Y. Miyako, and J. A. Mydosh, *Phys. Rev. Lett.* **83**, 5114 (1999).
- <sup>28</sup> K. Matsuda, Y. Kohori, T. Kohara, K. Kuwahara, and H. Amitsuka, *Phys. Rev. Lett.* **87**, 087203 (2001).
- <sup>29</sup> H. Amitsuka, K. Matsuda, I. Kawasaki, K. Tenya, M. Yokoyama, C. Sekine, N. Tateiwa, T. Kobayashi, S. Kawarazaki, and H. Yoshizawa, *J. Magn. Magn. Mater.* **310**, 214 (2007).
- <sup>30</sup> J. A. Mydosh and P. M. Oppeneer, *Rev. Mod. Phys.* **83**, 1301 (2011).
- <sup>31</sup> H. Amitsuka, K. Tenya, M. Yokoyama, A. Schenck, D. Andreica, F. Gygax, A. Amato, Y. Miyako, Y. Huang, and J. Mydosh, *Physica B* **326**, 418 (2003).
- <sup>32</sup> E. Hassinger, G. Knebel, K. Izawa, P. Lejay, B. Salce, and J. Flouquet, *Phys. Rev. B* **77**, 115117 (2008).
- <sup>33</sup> A. Villaume, F. Bourdarot, E. Hassinger, S. Raymond, V. Taufour, D. Aoki, and J. Flouquet, *Phys. Rev. B* **78**, 012504 (2008).
- <sup>34</sup> N. Nakashima, H. Ohkuni, Y. Inada, R. Settai, Y. Haga, E. Yamamoto, and Y. Onuki, *J. Phys.: Condens. Matter* **15**, S2011 (2003).
- <sup>35</sup> Y. J. Jo, L. Balicas, C. Capan, K. Behnia, P. Lejay, J. Flouquet, J. A. Mydosh, and P. Schlottmann, *Phys. Rev. Lett.* **98**, 166404 (2007).
- <sup>36</sup> E. Hassinger, G. Knebel, T. D. Matsuda, D. Aoki, V. Taufour, and J. Flouquet, *Phys. Rev. Lett.* **105**, 216409 (2010).
- <sup>37</sup> H. Yamagami and N. Hamada, *Physica B: Condens. Matter* **284**, 1295 (2000).
- <sup>38</sup> S. Elgazzar, J. Rusz, M. Amft, P. M. Oppeneer, and J. Mydosh, *Nat. Mater.* **8**, 337 (2009).
- <sup>39</sup> P. M. Oppeneer, J. Rusz, S. Elgazzar, M.-T. Suzuki, T. Durakiewicz, and J. A. Mydosh, *Phys. Rev. B* **82**, 205103 (2010).
- <sup>40</sup> V. P. Mineev and M. E. Zhitomirsky, *Phys. Rev. B* **72**, 014432 (2005).
- <sup>41</sup> C. M. Varma and L. Zhu, *Phys. Rev. Lett.* **96**, 036405 (2006).
- <sup>42</sup> K. Hanzawa, *J. Phys.: Condens. Matter* **19**, 072202 (2007).
- <sup>43</sup> A. R. Schmidt, M. H. Hamidian, P. Wahl, F. Meier, A. V. Balatsky, J. Garrett, T. J. Williams, G. M. Luke, and J. Davis, *Nature* **465**, 570 (2010).
- <sup>44</sup> S. Saitoh, S. Takagi, M. Yokoyama, and H. Amitsuka, *J. Phys. Soc. Jpn.* **74**, 2209 (2005).
- <sup>45</sup> S. Takagi, S. Ishihara, S. Saitoh, H. i. Sasaki, H. Tanida, M. Yokoyama, and H. Amitsuka, *J. Phys. Soc. Jpn.* **76**, 033708 (2007).
- <sup>46</sup> B. Lüthi, B. Wolf, P. Thalmeier, M. Günther, W. Sixl, and G. Bruls, *Phys. Lett. A* **175**, 237 (1993).
- <sup>47</sup> K. Kuwahara, H. Amitsuka, T. Sakakibara, O. Suzuki, S. Nakamura, T. Goto, M. Mihalik, A. A. Menovsky, A. d. Visser, and J. J. Franse, *J. Phys. Soc. Jpn.* **66**, 3251 (1997).
- <sup>48</sup> R. Okazaki, T. Shibauchi, and et al., *Science* **331**, 439 (2011).
- <sup>49</sup> T. Yanagisawa, S. Mombetsu, and et al., *Phys. Rev. B* **88**, 195150 (2013).
- <sup>50</sup> J. Buhot, M.-A. Méasson, Y. Gallais, M. Cazayous, G. Lapertot, D. Aoki, and A. Sacuto, *arXiv:1407.4651* (2014).
- <sup>51</sup> S. Tonegawa, K. Hashimoto, and et al., *Phys. Rev. Lett.* **109**, 036401 (2012).
- <sup>52</sup> S. Kambe, Y. Tokunaga, H. Sakai, T. D. Matsuda, Y. Haga, Z. Fisk, and R. E. Walstedt, *Phys. Rev. Lett.* **110**, 246406 (2013).
- <sup>53</sup> G. Motoyama, T. Nishioka, and N. K. Sato, *Phys. Rev. Lett.* **90**, 166402 (2003).
- <sup>54</sup> A. Amato, M. Graf, A. De Visser, H. Amitsuka, D. Andreica, and A. Schenck, *J. Phys.: Condens. Matter* **16**, S4403 (2004).
- <sup>55</sup> G. Motoyama, N. Yokoyama, A. Sumiyama, and Y. Oda, *J. Phys. Soc. Jpn.* **77**, 123710 (2008).
- <sup>56</sup> N. P. Butch, J. R. Jeffries, S. Chi, J. B. Leão, J. W. Lynn,



- and M. B. Maple, Phys. Rev. B **82**, 060408 (2010).
- <sup>57</sup> C. Bradley and A. Cracknell, *The Mathematical Theory of Symmetry in Solids* (OXFORD UNIVERSITY PRESS, 1972).
- <sup>58</sup> D. Khalyavin, S. Lovesey, A. Dobrynin, E. Ressouche, R. Ballou, and J. Flouquet, J. Phys.: Condens. Matter **26**, 046003 (2014).
- <sup>59</sup> A. V. Nikolaev and K. H. Michel, Phys. Rev. B **68**, 054112 (2003).
- <sup>60</sup> P. Erdős, G. Solt, A. Blaise, J. Fournier, and et al., Physica B+C **102**, 164 (1980).
- <sup>61</sup> W. Kopmann, F. Litterst, H.-H. Klauß, M. Hillberg, W. Wagener, G. Kalvius, E. Schreier, F. Burghart, J. Rebizant, and G. Lander, J. Alloy. Compd. **271**, 463 (1998).
- <sup>62</sup> M. Yoshizawa, D. Kimura, and et al., J. Phys. Soc. Jpn. **81**, 024604 (2012).
- <sup>63</sup> S. Tonegawa, S. Kasahara, and et al., Nat. Commun. **5**, 4188 (2014).
- <sup>64</sup> T. Mito, M. Hattori, G. Motoyama, Y. Sakai, T. Koyama, K. Ueda, T. Kohara, M. Yokoyama, and H. Amitsuka, J. Phys. Soc. Jpn. **82** (2013).
- <sup>65</sup> T. Hahn, U. Shmueli, A. J. C. Wilson, and E. Prince, *International tables for crystallography* (KLUWER ACADEMIC PUBLISHERS, 2002).
- <sup>66</sup> M.-T. Suzuki, N. Magnani, and P. M. Oppeneer, Phys. Rev. B **82**, 241103 (2010).
- <sup>67</sup> M.-T. Suzuki, N. Magnani, and P. M. Oppeneer, Phys. Rev. B **88**, 195146 (2013).
- <sup>68</sup> O. Gunnarsson and B. Lundqvist, Phys. Rev. B **13**, 4274 (1976).